

# Equivalent hyperon-nucleon interactions in low-momentum space

M. Kohno,<sup>1</sup> R. Okamoto<sup>2</sup>, H. Kamada<sup>2</sup> and Y. Fujiwara<sup>3</sup>

<sup>1</sup>*Physics Division, Kyushu Dental College,  
Kitakyushu 803-8580, Japan*

<sup>2</sup>*Department of Physics, Kyushu Institute of Technology,  
Kitakyushu 804-8550, Japan*

<sup>3</sup>*Department of Physics, Kyoto University,  
Kyoto 606-8502, Japan*

Equivalent interactions in a low-momentum space for the  $\Lambda N$ ,  $\Sigma N$  and  $\Xi N$  interactions are calculated, using the  $SU_6$  quark model potential as well as the Nijmegen OBEP model as the input bare interaction. Because the two-body scattering data has not been accumulated sufficiently to determine the hyperon-nucleon interactions unambiguously, the construction of the potential even in low-energy regions has to rely on a theoretical model. The equivalent interaction after removing high-momentum components is still model dependent. Because this model dependence reflects the character of the underlying potential model, it is instructive for better understanding of baryon-baryon interactions in the strangeness sector to study the low-momentum space  $YN$  interactions.

PACS numbers: 13.75.Ev, 21.30.-x

## I. INTRODUCTION

A low-momentum space nucleon-nucleon ( $NN$ ) interaction has been extensively studied in recent years [1, 2]. If we start with the full space realistic  $NN$  interaction, the discussion is focused on the evaluation of an effective  $NN$  interaction in a low-momentum space which reproduces the same eigenvalues or  $T$ -matrices in the low-momentum space as those of the original interaction. In this paper, we call such an effective interaction in a restricted space as an *equivalent interaction*. It was demonstrated [1] that after the high momentum components corresponding to short-range repulsion are renormalized, various  $NN$  potential models give essentially the same low-momentum  $NN$  interaction.

The construction of an energy-independent equivalent interaction in a model space has been one of the main subjects in effective interaction theories in various field. Okubo [3] proposed in 1950's a unitary transformation method to eliminate meson-degrees of freedom to obtain the  $NN$  potential. Through 1950's to 1970's, numerous theoretical works [4, 5, 6] have been devoted to nuclear many-body problems starting from realistic nucleon-nucleon interactions. In the context of the shell model effective interaction, Suzuki and Lee [7, 8] formulated a decoupling condition method using a similarity transformation and an iterative procedure to solve the decoupling equation. The theory behind recent developments is closely related to this viewpoint.

On the two-body level, the collapse of various realistic  $NN$  interactions to the universal interaction in a low-momentum space  $k \leq \Lambda$  with  $\Lambda \simeq 2 \text{ fm}^{-1}$  seems not to be surprising because of abundant  $NN$  scattering data in the corresponding energy region. In the strangeness non-zero sectors the scattering data is scarce at present, although studies of the hyperon-nucleon ( $YN$ ) and hyperon-hyperon ( $YY$ ) interactions have been accel-

erated with the experimental progress in hyper-nuclear physics. Thus the construction of the  $YN$  and  $YY$  potentials has to rely on a certain theoretical framework to a large extent. The Nijmegen group [9, 10, 11] has been revising the  $YN$  potentials on the basis of the one-boson exchange potential (OBEP) picture since the end of 1970's. The initial hard-core models [9] were replaced by the soft-core parameterization [10, 11]. The Jülich group [12, 13, 14] has also been developing another OBEP model. In spite of the basic flavor  $SU_3$  relations, there are still much uncertainties in the construction of the  $YN$  and  $YY$  potentials.

A different unified description was proposed for the octet baryon-baryon interactions by the Kyoto-Niigata group [15, 16] on the basis of an  $SU_6$  quark model, in which the gluonic interaction in the resonating group method (RGM) for two composite nucleons composed of three quarks is supplemented by the long-ranged one-boson exchange interaction between quarks. The most recent model fss2 [17] achieves comparable accuracy in the  $NN$  sector to modern realistic  $NN$  potentials. The advantage of the  $SU_6$  quark model is that the extension of the potential parameters determined in the  $NN$  sector to the strangeness  $S = -1$  and  $-2$  sectors seems to be less ambiguous than the OBEP models. Recently, a novel method based on the chiral effective field theory has been applied to the strangeness  $S = -1$  and  $S = -2$  baryon-baryon interactions [18, 19].

Because the present potential models for the  $YN$  interaction are not well regulated by experimental data, the equivalent interaction after removing the high-momentum components can still be model dependent. In other words, properties of these equivalent interactions reflect the character of the underlying potential model. Thus, it is interesting to compare the low-momentum space  $YN$  interactions obtained from different bare potential models.

The evaluation of low-momentum  $\Lambda N$  and  $\Sigma N$  interactions was recently reported by Schaefer *et al.* [20] for the momentum cut-off value of  $\Lambda \sim 2.5 \text{ fm}^{-1}$ , using several Nijmegen NSC potentials [11]. The new feature in the  $YN$  interactions is the presence, in most cases, of the coupling between two or three baryon-channels, such as  $\Lambda N$ - $\Sigma N$ ,  $\Xi N$ - $\Lambda\Lambda$ - $\Sigma\Sigma$ , and  $\Xi N$ - $\Sigma\Lambda$ - $\Sigma\Sigma$  couplings. In this paper, we present equivalent interactions in the low-momentum space with  $\Lambda = 2 \text{ fm}^{-1}$  for the  $\Lambda N$ ,  $\Sigma N$  and  $\Xi N$  potentials starting from the  $SU_6$  quark model bare potentials [17]. We choose this cut-off value as a typical low-momentum scale for which the potential model dependence is almost eliminated in the case of the  $NN$  interaction [1].

The naive definition of the potential based on the RGM formalism leads to an energy-dependent potential through the norm kernel. Such energy-dependence is not suited for the equivalent interaction theory. Recently, the method to eliminate the energy-dependence has been developed [21], using a renormalized RGM formalism. We use this prescription for the quark model potential. There is another complexity inherent in the RGM formulation of the baryon-baryon interaction, which is the presence of a Pauli forbidden state in certain channels. The interaction has to be applied in the space in which the Pauli forbidden state is projected out. In other words, an orthogonal condition to the forbidden state has to be imposed when solving the Schrödinger equation. This condition is not removed even if the energy-dependence is eliminated. Fortunately, however, on-shell and half-on-shell  $T$ -matrices are not influenced by the redundant component [22]. It is noted that the Pauli forbidden state appears only in the  $1S_0$  ( $11$ )s state in the model space of the baryon-octet baryon-octet interaction, specified by the Elliott notation  $(\lambda\mu)$ .

For the  $\Lambda N$  and  $\Sigma N$  cases, we also employ the Nijmegen NSC97f model. Our results with the NSC97f potential are mostly in accord with those shown by Schaefer *et al.* [20]. After removing high-momentum components, we still observe model dependence, in particular in  $\Sigma N$  channels. The comparison of the results with the quark model and the OBEP model demonstrates different characters of these potential models.

In Sec. II, we recapitulate the basics of the equivalent interaction theory in a model space. In the framework which was initiated by Suzuki and Lee [7, 8] and developed afterward by collaborators [23, 24] with including the generalization [25] to the case that the unperturbed model-space energies are non-degenerate, the mapping operator  $\omega$  which connects the model space  $P$  and the rest  $Q$  space plays an essential role to explicitly calculate the equivalent interaction. The mapping operator  $\omega$  is determined by the decoupling condition, which leads to a non-linear equation for  $\omega$ . This operator  $\omega$  can also be obtained by a linear equation by using the knowledge of the half-on-shell  $T$ -matrices, as derived by Epelbaum *et al.* [2]. We show, in Sec. II, a compact derivation of the linear equation. The actual evaluation of the equivalent

interaction can be carried out by discretizing the entire momentum space as was argued in the paper by Fujii *et al.* [26]. We extend this method to the case of  $YN$  interactions, in which there are couplings among several baryon-channels.

Results of numerical calculations are presented in Sec. III. We show only the diagonal matrix elements. Because the single-particle (s.p.) potential of the hyperon in infinite nuclear matter is determined by them in the lowest order, they can provide useful information about properties of the hyperon-nucleon interaction. We first give the results for the  $NN$  interaction for comparison, then present  $\Lambda N$  and  $\Sigma N$  equivalent interactions in the low-momentum space with  $\Lambda = 2 \text{ fm}^{-1}$  calculated both for fss2 and NSC97f. Equivalent interactions for  $\Xi N$  are evaluated only for fss2. Section IV summarizes the results of the present paper.

## II. EQUIVALENT INTERACTION

We recapitulate basic elements of the equivalent interaction theory, following the method by Suzuki and Lee [7, 8]. Let us denote the original Hamiltonian in the entire space by  $H = H_0 + V$ , and divide the full Hilbert space into a model space and the rest which are denoted by their relevant projection operators  $P$  and  $Q$ , respectively;  $P + Q = 1$ . In particular, the low-momentum space in the two-body problem is defined as  $P = \int_{|\mathbf{k}| < \Lambda} d\mathbf{k} |\mathbf{k}\rangle\langle\mathbf{k}|$ . The problem is to find the equivalent operator  $H_{eff}$  in the model space  $P$ , which reproduces the eigenvalue as those of the original  $H$ . A formal approach has been well known as the Feshbach projection method [5]. It is instructive to present the Schrödinger equation  $H|\Psi\rangle = E|\Psi\rangle$  in a matrix form.

$$\begin{pmatrix} PHP & PHQ \\ QHP & QHQ \end{pmatrix} \begin{pmatrix} P|\Psi\rangle \\ Q|\Psi\rangle \end{pmatrix} = E \begin{pmatrix} P|\Psi\rangle \\ Q|\Psi\rangle \end{pmatrix}. \quad (1)$$

It is straightforward to obtain the following equation in the model space  $P$  by eliminating  $Q\Psi$  in terms of  $Q\Psi = \frac{1}{E - QHQ} QHP\Psi$ :

$$P \left\{ H + HQ \frac{1}{E - QHQ} QH \right\} P\Psi = EP\Psi. \quad (2)$$

Thus  $H_{eff}$  can be identified with

$$H_{eff} = PH_0P + PVP + PVQ \frac{1}{E - QHQ} QVP. \quad (3)$$

In this case we obtain the energy-dependent effective interaction in the model space. This expression is rather formal, since it includes the energy  $E$  to be solved. It is pedagogical to remark that if  $V$  has the property of  $QVP = 0$  or  $PVQ = 0$ ,  $PH_0P + PVP$  is nothing but  $H_{eff}$  from the beginning.

Suzuki and Lee [7, 8] proposed in 1980 the way to construct the energy-independent equivalent potential in the

context of the similarity transformation. Their consideration serves as the basic for the recent development of various effective interaction theories. It is elementary to observe that the eigenvalues of the original Hamiltonian  $H$  do not change when  $H$  is transformed by a similarity transformation, namely by a regular matrix  $X$  and its inverse  $X^{-1}$  as  $H \Rightarrow H' \equiv X^{-1}HX$ . As noted above, if  $QX^{-1}HXP = 0$  holds,  $PX^{-1}HXP$  becomes the equivalent interaction in the model space  $P$ . Thus the task to find  $H_{eff}$  is reduced to determine  $X$  which satisfies  $QX^{-1}HXP = 0$ .

It is sufficient first to consider a regular matrix  $X$  in the following form.

$$X = \begin{pmatrix} 1, 0 \\ \omega, 1 \end{pmatrix}, \quad \text{then} \quad X^{-1} = \begin{pmatrix} 1, 0 \\ -\omega, 1 \end{pmatrix}. \quad (4)$$

The mapping matrix  $\omega = Q\omega P$ , which connects the  $P$  and  $Q$  spaces, plays a central role in the following. The decoupling condition  $QX^{-1}HXP = 0$  now reads:

$$QVP + QHQ\omega - \omega PHP - \omega PVQ\omega = 0. \quad (5)$$

Because this is a non-linear equation for  $\omega$ , we have to use some iteration method to solve it. Determining the mapping operator  $\omega$ , we obtain an energy-independent equivalent interaction in the model space  $P$  as  $PX^{-1}HXP = PH_0P + PV(1+\omega)P$ . This equivalent Hamiltonian is not hermitian at this stage. If we utilize a unitary matrix  $\tilde{X}$  in the following Okubo form [3, 23] constructed from  $\omega$  of Eq. (5) to transform the original  $H$ ,

$$\tilde{X} = \begin{pmatrix} 1, -\omega^\dagger \\ \omega, 1 \end{pmatrix} \begin{pmatrix} 1 + \omega^\dagger\omega, 0 \\ 0, 1 + \omega\omega^\dagger \end{pmatrix}^{-1/2}, \quad (6)$$

the equivalent Hamiltonian is apparently hermitian. The general argument of constructing an hermitian equivalent interaction was given in ref. [27]. It has to be stressed that other operators corresponding to physical observables are also transformed accordingly.

Although the equation (5) for  $\omega$  is non-linear, Epelbaum *et al.* showed in ref. [2] that the linear equation can be set up for the mapping operator  $\omega$  by the use of the half-on-shell  $T$ -matrices in the case of the two-body problem. This linear equation for  $\omega$  is easily derived in the above context as follows. By definition, the equivalent interaction in the  $P$  space  $H_0 + PV(1+\omega)P$  is to reproduce the original  $T$ -matrices in the  $P$  space. Namely we expect that the following equation should hold.

$$PTP = PV(1+\omega)P + PV(1+\omega)\frac{P}{\epsilon - H_0}TP, \quad (7)$$

where  $\epsilon$  is the on-shell energy and we are considering half-on-shell  $T$ -matrices. The original equation for  $T$  in the  $P$  space is

$$\begin{aligned} PTP &= PVP + PV\frac{1}{\epsilon - H_0}TP \\ &= PVP + PV\frac{P}{\epsilon - H_0}TP + PV\frac{Q}{\epsilon - H_0}TP \end{aligned} \quad (8)$$

Comparing Eq. (8) with Eq. (9), we obtain

$$PV\omega P + PV\omega\frac{P}{\epsilon - H_0}TP = PV\frac{Q}{\epsilon - H_0}TP \quad (9)$$

Taking out the common  $PVQ$ , we are led to the linear equation for  $\omega$ :

$$Q\omega P = \frac{Q}{\epsilon - H_0}TP - Q\omega\frac{P}{\epsilon - H_0}TP. \quad (10)$$

### III. RESULTS

When the role of the mapping operator  $\omega$  is figured out, we can devise a direct calculational procedure to determine  $\omega$ , as was explained as method-2 and used in Ref. [26]. The extension to the case in which several baryon-channels couple each other, e.g., the treatment of the  $\Lambda N$ - $\Sigma N$  transition, is straightforward. In principle, there is no difference in the calculational method for the tensor coupling and the baryon-channel coupling. We only have to enlarge the dimension of the relevant Hilbert space. It is noted that in the hyperon-nucleon interaction such a coupling between  $^1P_1$  and  $^3P_1$  channels also appears through the antisymmetric spin-orbit interaction which is absent in the  $NN$  case, although we do not examine the  $P$ -waves in the following.

We calculate equivalent  $\Lambda N$ ,  $\Sigma N$  and  $\Xi N$  matrix elements in the low-momentum space with the cut-off value of  $\Lambda = 2.0 \text{ fm}^{-1}$  for the  $^1S_0$  and  $^3S_1$  partial waves, starting from the Kyoto-Niigata  $SU_6$  quark model potential fss2 [17]. This momentum scale should be regarded as a representative one for which the potential model dependence of the description of high momentum components has been shown [1] to disappear in the case of the  $NN$  interaction. The Nijmegen NSC97f [11] is also used for the  $\Lambda N$  and  $\Sigma N$  interactions. These two potentials are especially different in the manner of constructing the short-range part. The Nijmegen OBEP model is based on the heavy meson exchange picture, while the quark model uses a RGM framework for nonrelativistic quark-clusters. As noted in Introduction, the energy-dependence from the RGM kernel is renormalized to give an energy-independent potential [21].

Although the calculational procedure is straightforward to treat the baryon-channel coupling, we have to be careful to interpret the matrix elements of the equivalent interaction in the  $P$  space. To obtain physically meaningful quantities such as hyperon s.p. energies in nuclear medium, we have to further solve the baryon-channel coupling problem in the  $P$  space. If the coupling effect in the  $P$  space is important, the matrix elements before solving the coupling problem give no clear physical insight. We encounter such a typical example in the  $\Xi N T = 1$  channel.

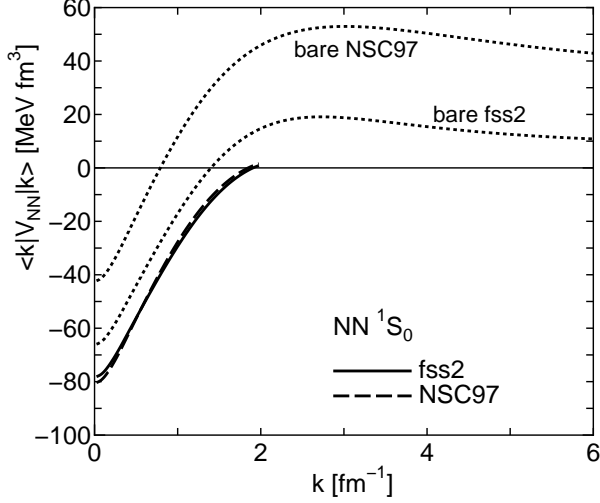


FIG. 1: Diagonal matrix elements of the equivalent interaction in the low-momentum space with  $\Lambda = 2 \text{ fm}^{-1}$  for the  $NN \ ^1S_0$  partial wave, using the quark model potential fss2 [17] and the Nijmegen potential NSC97 [11]. Bare matrix elements are shown by dotted curves.

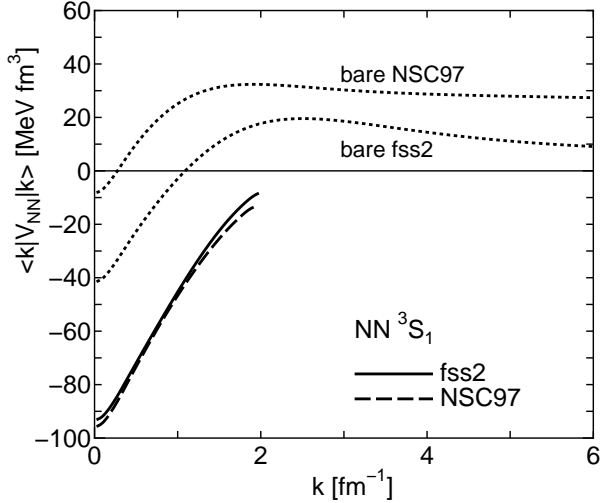


FIG. 2: Same as Fig. 1, but for the  $NN \ ^3S_1$  partial wave.

### A. $NN$ interaction

Before showing the equivalent interactions in the low-momentum space for the hyperon-nucleon sectors, we present results of the  $NN$  interaction for comparison. Diagonal matrix elements of the quark model potential fss2 [17] in the low-momentum space with  $\Lambda = 2 \text{ fm}^{-1}$  are shown by solid curves in Figs. 1 and 2 for  $^1S_0$  and  $^3S_1$ , respectively. These results are very close to those of the Nijmegen potential NSC97f depicted by dashed curves. It demonstrates that the quark model potential fss2 achieves the same level accuracy as modern realistic  $NN$  interactions, although the description at the short-range part is considerably different due to the RGM

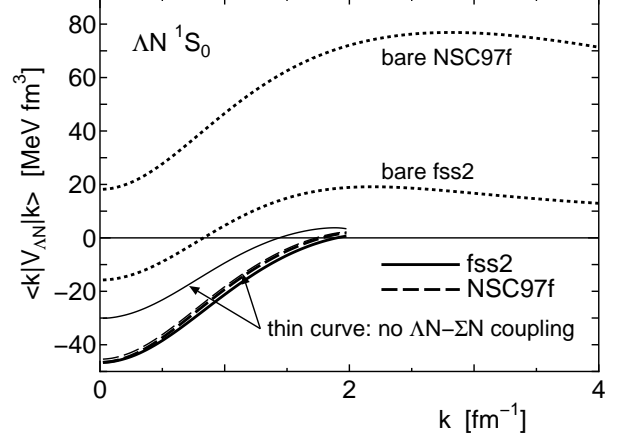


FIG. 3: Same as Fig. 1, but for the  $\Lambda N \ ^1S_0$  partial wave, using fss2 [17] and NSC97f [11]. Thin curves are results without  $\Lambda N$ - $\Sigma N$  coupling. Thick and thin curves for NSC97f are hard to be distinguished in the figure.

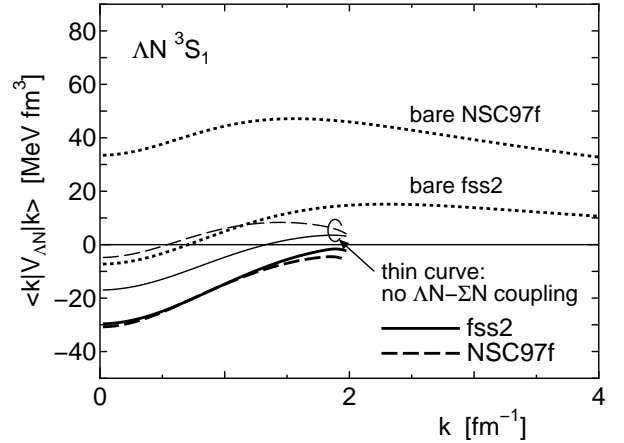


FIG. 4: Same as Fig. 3, but for the  $\Lambda N \ ^3S_1$  partial wave.

treatment. The thin curves in Figs. 1 and 2 for the bare matrix elements illustrate that the short-range repulsion of fss2 is rather moderate.

### B. $\Lambda N$ interaction

Properties of the  $\Lambda N$  interaction has been known empirically to some extent, based on the scattering data from bubble chamber experiments and the data of  $\Lambda$  hypernuclei in last 30 years. The central part is fairly well known from the universal depth of the  $\Lambda$ -nucleus potential of about 30 MeV, from light to heavy  $\Lambda$ -hypernuclei, while the non-central component is still ambiguous. Although the smallness of the  $\Lambda$  s.p. spin-orbit splitting in hypernuclei has been established experimentally [28], its relation to the two-body  $\Lambda N$  interaction has not been settled. One of the possible explanations has been offered by the quark model [17, 29] by pointing out the role

of the antisymmetric spin-orbit interaction which can almost cancel the contribution from the ordinary spin-orbit interaction. In this paper, however, we do not discuss this subject, because we present the results only for  $S$ -waves.

Figures 3 and 4 show the low-momentum space diagonal matrix elements of the equivalent  $\Lambda N$  interaction in the  $^1S_0$  and  $^3S_1$  channels with  $\Lambda = 2 \text{ fm}^{-1}$  together with bare matrix elements, both for the quark model potential fss2 [17] and the Nijmegen potential NSC97f [11]. In order to see the effects of the  $\Lambda N$ - $\Sigma N$  coupling, we also present results with turning off the coupling potential by the thin curves.

The Nijmegen potential and the quark model potential provide very similar matrix elements in the low-momentum space, though the bare matrix elements are different from each other, reflecting the different character in the short-range part. Again the short-range repulsion of fss2 is moderate.

In the  $^1S_0$  channel, the effect of the  $\Lambda N$ - $\Sigma N$  coupling is seen to be negligibly small for NSC97f. Because the pion-exchange is absent in this partial wave, the  $\Lambda N$ - $\Sigma N$  coupling is expected to be weak. In the quark model description, the situation is somewhat different. In the RGM treatment of the two quark-clusters the Pauli forbidden state appears in this  $^1S_0$   $\Lambda N$ - $\Sigma N$  channel. When the  $\Lambda N$ - $\Sigma N$  coupling is switched off, the orthogonality to the Pauli forbidden state on the quark level is not strictly satisfied, which may cause an artificial coupling effect observed in Fig. 3. This feature deserves future investigation. The  $^3S_1$  channel is free from the Pauli forbidden state. Comparing the thick and thin curves in Fig. 4, we see that the considerable amount of the attractive contribution comes from the  $\Lambda N$ - $\Sigma N$  coupling in the outer space beyond  $\Lambda = 2 \text{ fm}^{-1}$ .

It is remarkable to see that the two potential models give almost identical diagonal matrix elements in the low-momentum space both for  $^1S_0$  and  $^3S_1$  channels, though the bare matrix elements are different. This implies that the potential model for the  $\Lambda N$   $S$ -wave interaction is now almost under control. The study of  $P$ -waves, in particular the magnitude of the spin-orbit and antisymmetric spin-orbit components, is an important future subject. The careful study of  $\Lambda N$ - $\Sigma N$  coupling effects, including those within the low-momentum space, is also required, because hypernuclear  $\gamma$ -spectroscopic measurements [28] with the accuracy of the order of keV are beginning to provide the data of excitation spectrum of  $\Lambda$  hypernuclei.

### C. $\Sigma N$ interaction

The  $\Sigma N$  interaction has been expected to have specific spin and isospin dependences. Harada *et al.* [30] demonstrated that the net attractive interaction in the  $^1S_0$   $T = 3/2$  channel can yield the bound  $^4_\Sigma\text{He}$  hypernucleus with  $J^\pi = 0^+$ , which corresponds to the experimental observation in the  $^4\text{He}(K^-, \pi^-)$  reactions with the stopped kaon [31] as well as the kaon in flight [32]. How-

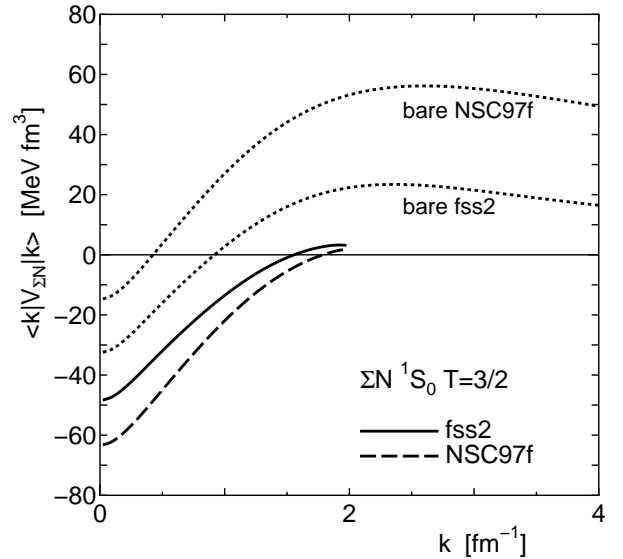


FIG. 5: Same as Fig. 1, but for the  $\Sigma N$   $^1S_0$  partial wave, using fss2 [17] and NSC97f [11]. In this partial wave, there is no baryon-channel coupling.

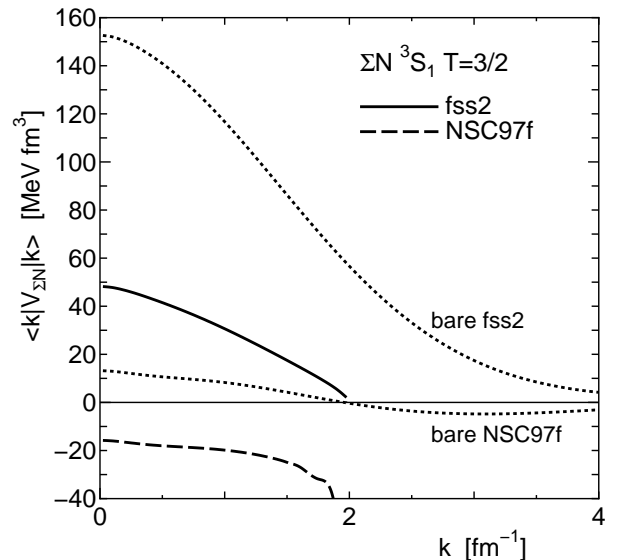


FIG. 6: Same as Fig. 5, but for the  $\Sigma N$   $^3S_1$   $T = 3/2$  partial wave. In this partial wave, there is no baryon-channel coupling.

ever, probably due to the repulsion in the  $^3S_1$   $T = 3/2$  channel,  $\Sigma$  bound states are unlikely in heavier nuclei, which has been supported by experimental results on targets  $^6\text{Li}$  and  $^9\text{Be}$  [33].

The quark model picture has been known from the earlier studies [29] to give a definite prediction that certain partial waves such as the  $\Sigma N$   $^3S_1$   $T = 3/2$  state should be strongly repulsive due to the quark Pauli effect, which has no explicit counterpart in the OBEP model. The character related to the Pauli effect might be uncovered

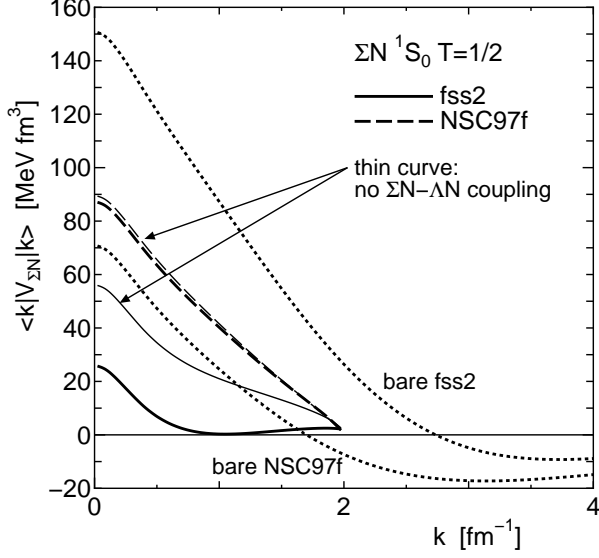


FIG. 7: Same as Fig. 5, but for the  $\Sigma N$   $^1S_0$   $T = 1/2$  partial wave. Thin curves are results without the  $\Lambda N$ - $\Sigma N$  coupling.

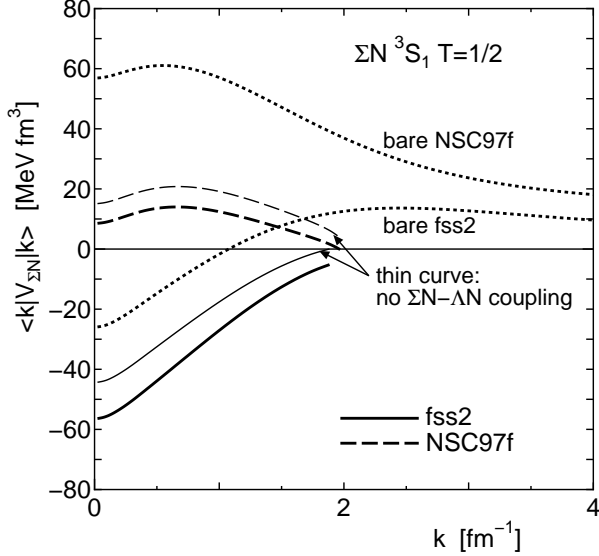


FIG. 8: Same as Fig. 5, but for the  $\Sigma N$   $^3S_1$   $T = 1/2$  partial wave. Thin curves are results without the  $\Lambda N$ - $\Sigma N$  coupling.

in the low-momentum space equivalent interaction.

The  $T = 3/2$  channels have no  $\Sigma N$ - $\Lambda N$  coupling because the  $\Lambda$  hyperon is isosinglet. Figure 5 shows the diagonal matrix elements of the low-momentum space equivalent  $\Sigma N$  interaction in the  $^1S_0$   $T = 3/2$  channel. Results for fss2 [17] and NSC97f [11] are shown by the solid and dashed curves, respectively, while bare matrix elements up to  $k = 4 \text{ fm}^{-1}$  are shown by the dotted curves. The tendency of how high-momentum components are renormalized is similar to the  $NN$   $^1S_0$  case. The attractive interaction in this channel is important for the existence of the bound  $^4_2\text{He}$  state. The quark model

potential is sufficiently attractive to yield the bound state as the Nijmegen potential does. In the viewpoint of the quark model [17], the flavor  $SU_3$  symmetry tells that this channel is dictated by the (22) symmetric component of the Elliott notation  $(\lambda\mu)$ . This component is the same as in the  $^1S_0$  ( $T = 1$ )  $NN$  state, and thus the rather strong attractive character after renormalizing high-momentum components is reasonable.

Quantitatively different results are obtained between fss2 and NSC97f in the  $^3S_1$   $T = 3/2$  channel, which are shown in Fig. 6. The quark model potential predicts repulsive interaction, which comes from the quark Pauli effect. The correlation due to the Pauli effect is not so short-ranged, as the magnitude of the matrix element at  $k = 4 \text{ fm}^{-1}$  indicates. The repulsive character persists in the low-momentum space. On the other hand, the NSC97f model does not have strong repulsion and the low-momentum equivalent interaction is attractive. Owing to the spin and isospin weight factors, this  $^3S_1$   $T = 3/2$  state dominantly contributes to the  $\Sigma$  s.p. potential in nuclear medium. Analyses [34, 35, 36] of the  $(\pi^-, K^+)$   $\Sigma$  formation inclusive spectra [34] have indicated that the  $\Sigma$ -nucleus mean field is repulsive.

Figure 7 shows results for the  $^1S_0$   $T = 1/2$  state. The thin solid curve presents the result for which the  $\Sigma N$ - $\Lambda N$  channel-coupling is neglected. The corresponding result for NSC97f is shown by the dashed curve. Bare matrix elements are also shown up to  $k = 4 \text{ fm}^{-1}$ . Both potential models predict repulsive interaction in this channel. As we have already seen in the  $\Lambda N$  interaction, the  $\Sigma N$ - $\Lambda N$  channel-coupling effect is very weak in NSC97f. It is noteworthy that the diagonal matrix elements in the low-momentum space become more repulsive in NSC97f when renormalizing the high-momentum attractive components.

Figure 8 shows results for the  $^3S_1$   $T = 1/2$  state. Here we see characteristic difference for the prediction of the  $\Sigma N$ - $\Lambda N$  coupling effect between fss2 and NSC97f. The behavior of the diagonal matrix elements with fss2 resembles that of the  $NN$   $^3S_1$  state given in Fig. 2. In fact, from the flavor  $SU_3$  symmetry this channel has a (03) component by 50%, which is the component of the  $NN$   $^3S_1$  interaction. Because the other half component of the  $(11)_a$  gives a minor contribution, the  $\Sigma N$  interaction in the  $^3S_1$   $T = 1/2$  state should be similar to the  $NN$   $^3S_1$  interaction in the quark model description. In contrast, weakly repulsive matrix elements are seen for the  $^3S_1$   $T = 1/2$   $\Sigma N$ - $\Sigma N$  interaction from NSC97f. It has to be remarked, however, that the  $\Sigma N$ - $\Lambda N$  coupling in the  $P$  space, which is not yet taken into account, can change even the sign of the diagonal matrix elements. In fact,  $G$ -matrix calculations [37] in symmetric nuclear matter with using NSC97f tells that the contribution from this channel to the  $\Sigma$  s.p. potential in nuclear medium is attractive and becomes repulsive if we switch off the  $\Sigma N$ - $\Lambda N$  coupling. This fact simply means that we have to be careful to interpret the matrix elements in the case that there exist coupling channels and the coupling effect is

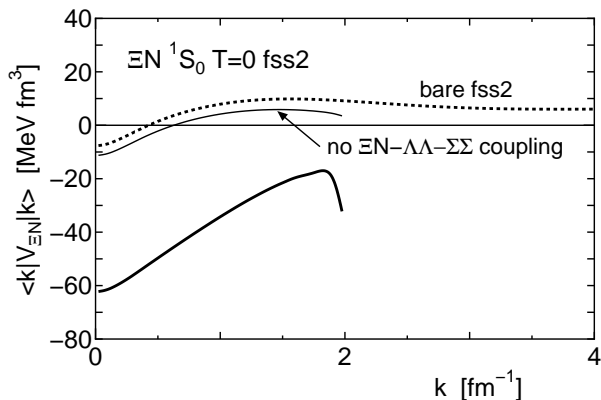


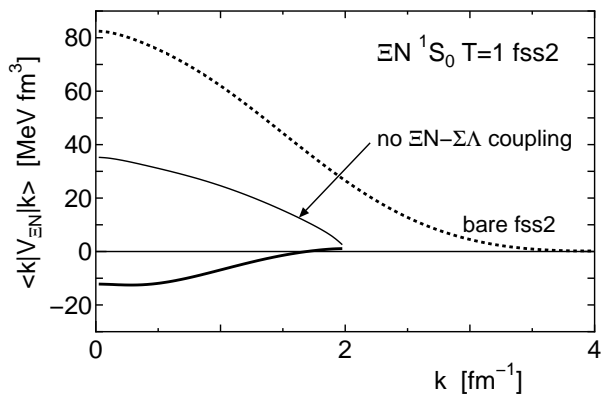
FIG. 9: Diagonal matrix elements of the equivalent interaction in the low-momentum space with  $\Lambda = 2 \text{ fm}^{-1}$  for the  $\Xi N \ ^1S_0 \ T=0$  partial wave, using fss2 [17]. Bare matrix elements are shown by a dotted curve. The thick and thin curves are results with and without taking into account the  $\Xi N$ - $\Lambda\Lambda$ - $\Sigma\Sigma$  channel coupling, respectively.

important in the low-momentum space. We encounter such a situation also in the  $\Xi N \ ^1S_0 \ T=1$  state.

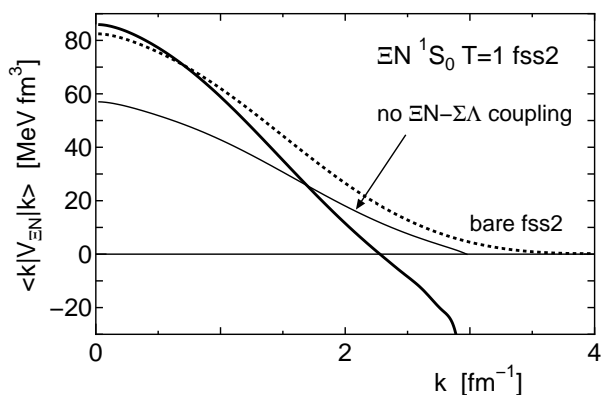
#### D. $\Xi N$ interaction

There are two kinds of sources for the experimental information about the baryon-baryon interaction in the strangeness  $S = -2$  sector. One is the estimation of a  $\Xi$ -nucleus s.p. potential from DWIA analyses [38] of the  $(K^-, K^+)$   $\Xi^-$  formation spectra on  $^{12}\text{C}$ . The tentative conclusion is that the depth of the s.p. potential is about 14 MeV. The other clue is the strength of the  $\Lambda\Lambda$  attraction through binding energies of double- $\Lambda$  hypernuclei. The recent discovery of  ${}_{\Lambda\Lambda}^6\text{He}$  [39] has indicated that the attraction of the  $\Lambda\Lambda$  interaction is rather weak. There is also an attempt [40] to measure the  $\Xi N \rightarrow \Lambda\Lambda$  inelastic cross section and deduce the  $\Lambda\Lambda$  correlation in the  $\Xi$  formation reaction. Nevertheless all these experimental data are in the rudimentary stage and far from sufficiently constraining the interactions which have a variety of baryon-channel couplings. Thus the investigation using theoretical models of the  $\Xi N$  interaction is important.

Because the computer code for the Nijmegen  $\Xi N$  interaction was not available, we present results only with the Kyoto-Niigata quark model potential fss2 [17]. Figure 9 shows the low-momentum space equivalent  $\Xi N$  interaction in the  $^1S_0 \ T=0$  state with  $\Lambda = 2 \text{ fm}^{-1}$  together with the bare matrix elements up to  $k = 4 \text{ fm}^{-1}$ . If the coupling to the  $\Lambda\Lambda$ - $\Sigma\Sigma$  channel is neglected, the diagonal matrix element of the equivalent interaction in the low-momentum space is close to that of the bare interaction, which indicates that the correlation in the  $\Xi N$ - $\Xi N$  channel itself is rather weak. The result of the large attraction in the  $\Xi N$  interaction in the low-momentum



(a)



(b)

FIG. 10: Same as Fig. 9, but for the  $\Xi N \ ^1S_0 \ T=1$  partial wave. (a) with  $\Lambda = 2 \text{ fm}^{-1}$  and (b) with  $\Lambda = 3 \text{ fm}^{-1}$ . The thick and thin curves are results with and without taking into account the  $\Xi N$ - $\Sigma\Lambda$  channel coupling, respectively.

space originates from the baryon-channel coupling effect. Among other  $S$ -waves, this channel turns out to be most attractive. As noted in the previous section, however, it is necessary to explicitly treat the  $\Xi N$ - $\Lambda\Lambda$ - $\Sigma\Sigma$  coupling in the  $P$  space in order to obtain more physically meaningful information.

The  $^1S_0 \ T=1$  state is shown in Fig. 10(a). In this state the  $\Sigma\Sigma$  channel is not allowed and the  $\Xi N$  state couples only with the  $\Sigma\Lambda$  state. Looking at the matrix elements at large  $k$ , we observe that the short-range repulsion is weak in this  $\Xi N$ - $\Xi N$  channel. It is found in this channel that because the baryon-coupling effect is strong, the sign of the diagonal matrix elements does not indicate the property of the interaction. For example, we show, in Fig. 10(b), the diagonal matrix elements of the low-momentum equivalent interaction with the cut-off value of  $\Lambda = 3 \text{ fm}^{-1}$ . In this case  $\Xi N$ - $\Xi N$  diagonal matrix elements are mostly positive. In between  $\Lambda = 3 \text{ fm}^{-1}$  and  $2 \text{ fm}^{-1}$ , the diagonal matrix elements change sign, which suggests that the baryon-channel coupling effects in the  $P$  space are decisively important, and thus the  $\Xi N$  and  $\Sigma\Lambda$  states are strongly mixed.

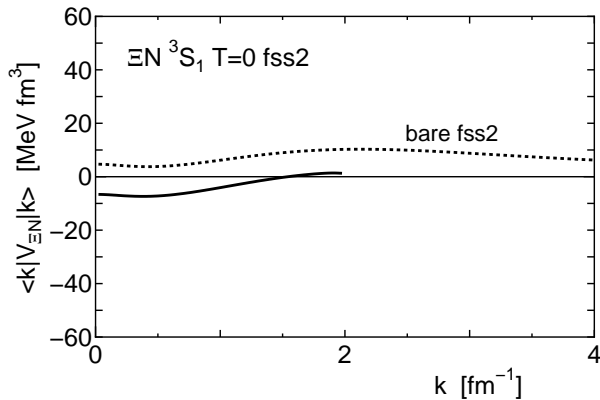


FIG. 11: Same as Fig. 9, but for the  $\Xi N$   ${}^3S_1$   $T=0$  partial wave. In this partial wave, there is no baryon-channel coupling.

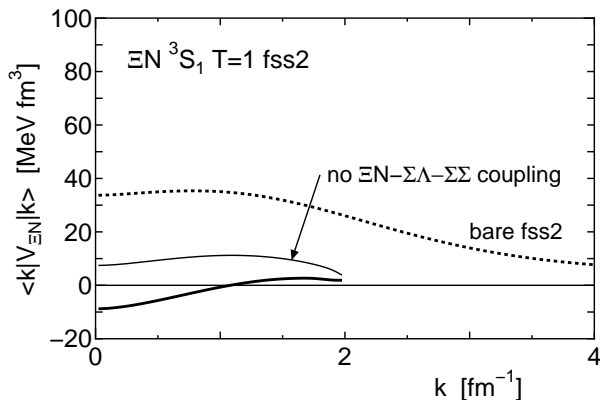


FIG. 12: Same as Fig. 9, but for the  $\Xi N$   ${}^3S_1$   $T=1$  partial wave. The thin curve shows results without taking into account the  $\Xi N$ - $\Sigma\Lambda$ - $\Sigma\Sigma$  channel coupling.

The  ${}^3S_1$   $T=0$  state is classified to the pure  $(11)_a$  state in the flavor  $SU_3$  symmetry and no baryon-channel coupling appears in this state. The quark model [17] predicts that the bare  $\Xi N$  interaction is already weak. Figure 11 shows that the low-momentum equivalent  $\Xi N$  interaction in this partial wave becomes slightly attractive.

As is shown in Fig. 12, the quark model potential fss2 predicts that the  $\Xi N$  interaction in the  ${}^3S_1$   $T=1$  state is also not so strong. Due to the  $\Xi N$ - $\Sigma\Lambda$ - $\Sigma\Sigma$  coupling the diagonal matrix elements of the low-momentum equivalent  $\Xi N$  interaction can be slightly negative.

Altogether, the quark model potential fss2 [17] predicts that the  $\Xi N$  interactions in  ${}^3S_1$  channels are weak. For the estimation of the  $\Xi$ -nucleus s.p. potential in nuclear medium, we expect an attractive contribution from the  ${}^1S_0$   $T=0$  state but a repulsive contribution from the  ${}^1S_0$   $T=1$  state. Higher partial waves may play an important role for the  $\Xi$ -nucleus s.p. potential.

#### IV. CONCLUSIONS

We have calculated low-momentum space equivalent interactions for hyperon-nucleon interactions, starting from two models of the bare potentials, the quark model potential fss2 [17] and the Nijmegen OBEP model NSC97f [11]. An effective interaction in a restricted space which reproduces the same eigenvalues or  $T$ -matrices in that space as those of the original full-space interaction is named as an equivalent interaction in this paper.

The quark model potential uses a RGM framework, thus the naive definition of the baryon-baryon interaction on the basis of the RGM Born kernel is energy-dependent. Recently, the technique to eliminate the energy-dependence was developed [21]. We have used this prescription for the quark model potentials for the octet baryon-baryon interactions. The calculation of the low-momentum space equivalent interaction for the quark model potential is interesting in two aspects. One is related to the different non-local character from that of the one-boson exchange picture, especially at short distance due to the RGM treatment of two quark-composite clusters. Another point is that the extension of the potential to the strangeness  $S=-1$  and  $S=-2$  sectors based on the parameters fixed in the  $NN$  sector has been shown [17] to be less ambiguous than the OBEP model. It is useful to elucidate the similarity and the difference in the  $\Lambda N$ ,  $\Sigma N$  and  $\Xi N$  interactions between the quark model and the Nijmegen model. As the representative potential for the latter model, we have employed the NSC97f [11], which was used in the similar calculations recently reported by Schaefer *et al.* [20].

The merit of considering the low-momentum space equivalent interaction for the  $YN$  interactions is to eliminate the model dependent characters at short distance, as has been demonstrated for the  $NN$  case by Bogner *et al.* [1]. Thus we can concentrate on features of the  $YN$  interaction relevant to low-energy experimental hypernuclear observables.

First we have presented the  $NN$  results for the sake of the comparison. The quark model potential gives almost the same results as other modern realistic  $NN$  potentials, as it should. The  $\Lambda N$  equivalent interaction in the low-momentum space turns out to be almost identical in the quark model and the OBEP model. This is probably because we have some amount of constraints from  $\Lambda$  hypernuclear data in addition to old scattering data.

Experimental data for the  $\Sigma N$  interaction is very limited. Thus the model dependence in the theoretical construction of the  $\Sigma N$  potential is large. In fact, the quark model and the Nijmegen OBEP model provide different equivalent interactions in the low-momentum space. In particular, we note that the quark model predicts repulsion in the  ${}^3S_1$   $T=3/2$  state which originates from the Pauli effect on the quark level, while the NSC97f potential expects attraction. On the other hand the repulsive contribution of NSC97f in the  ${}^1S_0$   $T=1/2$  state is rather strong.



The  $\Xi N$  interaction is less known experimentally. This subject is one of the primary subjects of the on-going J-PARC project [41]. The matrix elements in the low-momentum space from the quark model potential suggests that the  $\Xi$ -nucleus s.p. potential is probably attractive due to the interaction in the  $^1S_0$  state in the isospin  $T = 0$  channel, but weak. It is expected that there are strong baryon-channel coupling effects both in the high-momentum space and in the low-momentum space. In this paper, we do not consider higher partial waves. Actually they may be important for the quantitative discussion of the  $\Xi$  hyperon in nuclear medium. These are the future subjects to study.

In hyperon-nucleon interactions, baryon-channel couplings appear in most cases. If the coupling effect is important, as in the case of the  $\Sigma N$   $^3S_1$   $T = 1/2$  state

in the Nijmegen NSC97f model and the  $\Xi N$   $^1S_0$   $T = 1$  state in the quark model, we have to solve the channel-coupling problem in the low-momentum space in order to obtain physically meaningful quantities. When considering hyperons in nuclear medium, we also have to take into account the Pauli exclusion effect on the hadron level in a nuclear many body system. The effect of the three-body correlation through the coupling of the Pauli effect and the elimination of the high momentum components of the interaction may be important for hyperons in nuclear medium.

This study is supported by Grants-in-Aid for Scientific Research (C) from the Japan Society for the Promotion of Science (Grant Nos. 17540263 and 18540261).

- 
- [1] S.K. Bogner, T.T.S. Kuo, and A. Schwenk, Phys. Rep. **386**, 1 (2003).
- [2] E. Epelbaum, W. Glöckle, A. Krüger, and Ulf-G. Meißner, Nucl. Phys. **A645**, 413 (1999).
- [3] S. Okubo, Prog. Theor. Phys. **12**, 603 (1954)
- [4] C. Bloch and J. Horowitz, Nucl. Phys. **8**, 91 (1958).
- [5] H. Feshbach, Ann. Phys. **5**, 357 (1958).
- [6] B.H. Brandow, Rev. Mod. Phys. **39**, 771 (1967).
- [7] K. Suzuki and S.Y. Lee, Prog. Theor. Phys. **64**, 2091 (1980).
- [8] S.Y. Lee and K. Suzuki, Phys. Lett. **91B**, 173 (1980).
- [9] M.M. Nagels, T.A. Rijken and J.J. de Swart, Phys. Rev. D **12**, 744(1975); D **15** (1977), 2547; D **20**, 1633 (1979).
- [10] P.M.M. Maessen, T.A. Rijken and J.J. de Swart, Phys. Rev. C **40**, 2226 (1989).
- [11] T.A. Rijken, V.G.J. Stoks, and Y. Yamamoto, Phys. Rev. **C59**, 21 (1999).
- [12] B. Holzenkamp, K. Holinde and J. Speth, Nucl. Phys. **A500**, 485 (1989).
- [13] A. Reuber, K. Holinde and J. Speth, Nucl. Phys. **A570**, 543 (1994).
- [14] J. Haidenbauer and Ulf-G. Meißner, Phys. Rev. **C72**, 044005 (2005).
- [15] Y. Fujiwara, C. Nakamoto and Y. Suzuki, Phys. Rev. Lett. **76**, 2242 (1996).
- [16] Y. Fujiwara, C. Nakamoto and Y. Suzuki, Phys. Rev. C **54**, 2180 (1996).
- [17] Y. Fujiwara, Y. Suzuki, and C. Nakamoto, Prog. Part. Nucl. Phys. **58**, 439 (2007).
- [18] H. Polinder, J. Haidenbauer and Ulf-G. Meißner, Nucl. Phys. **A779**, 244 (2006).
- [19] H. Polinder, J. Haidenbauer and Ulf-G. Meißner, nucl-th/0705.3753.
- [20] B.-J. Schaefer, M. Wagner, J. Wambach, T.T.S. Kuo, and G.E. Brown, Phys. Rev. **C73**, 011001(R) (2006).
- [21] Y. Suzuki, H. Matsumura, M. Orabi, Y. Fujiwara, P. Descouvemont, M. Theeten and D. Baye, in preparation.
- [22] Y. Fujiwara, M. Kohno, C. Nakamoto and Y. Suzuki, Prog. Theor. Phys. **104**, 1025 (2000).
- [23] K. Suzuki, Prog. Theor. Phys. **68**, 246 (1982).
- [24] K. Suzuki and R. Okamoto, Prog. Theor. Phys. **70**, 439 (1983).
- [25] K. Suzuki, R. Okamoto, P. J. Ellis, T. T. S. Kuo, Nucl. Phys. **A567**, 576 (1994).
- [26] S. Fujii, E. Epelbaum, H. Kamada, R. Okamoto, K. Suzuki and W. Glöckle, Phys. Rev. **C70**, 024003 (2004).
- [27] R. Okamoto, S. Fujii and K. Suzuki, Int. J. Mod. Phys. **14**, 21 (2005).
- [28] O. Hashimoto and H. Tamura, Prog. Part. Nucl. Phys. **57**, 564 (2006).
- [29] M. Oka, K. Shimizu and K. Yazaki, Nucl. Phys. **A464**, 700 (1987).
- [30] T. Harada, S. Shinmura, Y. Akaishi, and H. Tanaka, Nucl. Phys. **A507**, 715 (1990).
- [31] R.S. Hayano *et al.*, Phys. Lett. **B231**, 355 (1989).
- [32] T. Nagae *et al.*, Phys. Rev. Lett. **80**, 1605 (1998).
- [33] S. Bart *et al.*, Phys. Rev. Lett. **83**, 5238 (1999).
- [34] H. Noumi *et al.*, Phys. Rev. Lett. **89**, 072301 (2002); **90**, 049902(E) (2003).
- [35] T. Harada and Y. Hirabayashi, Nucl. Phys. **A759**, 143 (2005).
- [36] M. Kohno, Y. Fujiwara, Y. Watanabe, K. Ogata and M. Kawai, Phys. Rev. **C74**, 064613 (2006).
- [37] M. Kohno, Y. Fujiwara, T. Fujita, C. Nakamoto and Y. Suzuki, Nucl. Rev. **A674**, 229 (2000).
- [38] P. Khaustov *et al.*, Phys. Rev. **C61**, 054603 (2000).
- [39] H. Takahashi *et al.*, Phys. Rev. Lett. **87**, 212502 (2001).
- [40] J.K. Ahn *et al.*, Phys. Lett. **B633**, 214 (2006).
- [41] T. Nagae, *Proc. of Int. Nucl. Phys. Conf.*, Tokyo, Japan, 3-8 June, 2007.